Available online at www.sciencedirect.com
SCIENCE DIRECT®
Pattern Recognition Letters 27 (2006) 1191–1200
Pattern Recognition Letters
www.elsevier.com/locate/patrec

A fast and accurate approach for 3D image registration using the scatter search evolutionary algorithm ☆

O. Cordón [a], S. Damas [b], J. Santamaría [b,*]

[a] Department of Computer Science and Artificial Intelligence, E.T.S.I. Informatica, University of Granada, C/Daniel Saucedo Aranda, s/n, 18071 Granada, Spain
[b] Department of Software Engineering, University of Granada, Granada, Spain

Available online 4 January 2006

Abstract

Nowadays, image registration (IR) is still an important and useful task in several areas such as remote sensing, medicine, cartography, and computer vision. Different approaches to solve the existing variants of the problem are commonly proposed in the specialized literature. In this paper, we focus our interest on the 3D IR problem considering similarity transformations and our proposal is based on the use of a new procedure based on the evolutionary computation framework for non-linear optimization. We apply an emergent global optimization strategy called scatter search providing a fast and accurate algorithm. To measure its performance, we design an experimental setup considering some of the most accepted and accurate classical and evolutionary techniques for the problem, as well as six different shapes, one synthetic and five magnetic resonance images, dealing with different levels of noise and occlusion in the scenarios treated.

Keywords: Image registration; Evolutionary computation; Scatter search; Genetic algorithms; Iterative closest point

1. Introduction

Image registration (IR) is a fundamental task in computer vision used to finding a correspondence (or transformation) among two or more pictures taken under different conditions: at different times, using different sensors, from different viewpoints, or a combination of them (Brown, 1992; Zitová and Flusser, 2003). On the other hand, evolutionary computation (EC) (Bäck et al., 1997) uses computational models of evolutionary processes as key elements in the design and implementation of computer-based problem solving systems. Genetic algorithms (GAs) (Holland, 1975) are maybe the most known evolutionary algorithms.

In the last few years, there is an increasing interest on applying EC fundamentals to IR (Chow et al., 2004; Cordón et al., 2003; Garai and Chaudhuri, 2002; Han et al., 2001; He and Narayana, 2002; Yamany et al., 1999). Unfortunately, we can find a lack of accuracy when facing this problem and different contributions fall into simplifications. On the one hand, when only 2D rotations and translations are considered in order to define the geometric transformation involved in the IR problem (see Section 2.1), the extension of the obtained results to more complex real scenarios is limited. Even worse, other proposals do not apply EC concepts in the more suitable way: either using an improper coding scheme of solutions and/or applying obsolescent evolutionary mechanisms (see Section 3).

In this work, we try to exploit the benefits of applying *scatter search* (SS) (Laguna and Martí, 2003) to solve the 3D IR problem. Unlike GAs, SS components are designed considering a deterministic non-randomized scenario, encouraging a tradeoff between search intensification and

☆ This work was supported by the Spanish Ministerio de Ciencia y Tecnología under project TIC2003-00877 (including FEDER fundings).
* Corresponding author. Tel.: +34 958246143; fax: +34 958243317.
E-mail addresses: ocordon@decsai.ugr.es (O. Cordón), sdamas@ugr.es (S. Damas), jsantam@ugr.es (J. Santamaría).

0167-8655/$ - see front matter © 2005 Elsevier B.V. All rights reserved.
doi:10.1016/j.patrec.2005.07.017

diversification. Hence, our intention is to provide a faster and more accurate algorithm than those in the IR literature. In particular, we aim at ensuring a better accuracy than the technique described in (Chow et al., 2004) which randomly discards a huge amount of image data to achieve a quicker but somehow inaccurate registration estimation (see Section 3).

To do so, we rely on: (i) the use of a spatial indexed structure (the grid closest point (GCP) (Yamany et al., 1999)) in order to obtain an efficient estimation of the distance between points; (ii) the use of a population size several times lower than the one typically defined with GAs; (iii) the generation of an initial population spread throughout the search space, in order to encourage diversification; (iv) the establishment of a systematic solution combination criterion to favor the search space intensification; and (v) the use of local search to achieve a faster convergence to promising solutions (see Section 4).

The paper structure is as follows. In Section 2 we give some IR basics. Next, we make a critical review of the existing evolutionary approaches to the IR problem in Section 3. Section 4 describes our proposal, which is tested in Section 5 over different images and transformations, confronted with some of the most accepted and recent proposals in the IR literature (Chow et al., 2004; Liu, 2004; Yamany et al., 1999). Finally, in Section 6 we present some conclusions and new open lines for future works.

2. Image registration

In this section we present an IR overview: Section 2.1 briefly introduces some IR basics, while Section 2.2 reviews the different existing IR approaches.

2.1. IR basics

There is not an universal design for a hypothetical IR method that could be applicable to all registration tasks, because various considerations of the particular application must be taken into account. Nevertheless, IR methods require the four following components: two input *Images*, named as Scene $I_s = \{\vec{p}_1, \vec{p}_2, \ldots, \vec{p}_n\}$ and Model $I_m = \{\vec{p}'_1, \vec{p}'_2, \ldots, \vec{p}'_m\}$, with $\vec{p}_i, \vec{p}'_j$ being the image points; a *Registration transformation* f, which is a parametric function relating both images; a *Similarity metric function* F (see Section 4.2), in order to measure a qualitative value of *closeness/resemblance* between the scene and the model images; and an *Optimizer* which looks for the optimal transformation within the definition interval of each f parameter.

Likewise, IR is the process of finding the optimal spatial transformation f achieving the best fitting (measured using F) between the model and the transformed scene points, $F(f(\vec{p}_i), \vec{p}'_j)$, where $\{f(\vec{p}_i), \vec{p}'_j\}$ is a point matching. Such a transformation estimation is interpreted into an iterative optimization process in order to properly explore the search space (Fig. 1).

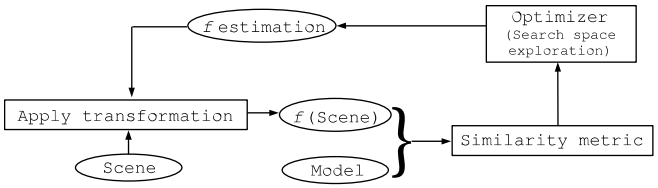

Fig. 1. The IR optimization process.

We can sort the different kinds of transformations f according to the maintenance (or not) of an established relation between the points in both the scene and the model images, i.e., if f is a *similarity transformation*, every angle in the scene is preserved and the relative change in segment dimensions is the same in all directions, after applying it. Hence, a similarity transformation can be split in three ones: translation, rotation and uniform scaling (see Section 4.2). Other examples of f transformations are the affine, projective, and elastic (Brown, 1992).

Orders of magnitude in the scale of f parameters are crucial when solving registration problems. Unit changes in angle have a much greater impact on an image than unit changes in translation. This difference in scale appears as elongated valleys in the parameter search space causing difficulties for the traditional local optimizers (Besl and McKay, 1992; He and Narayana, 2002). Moreover, inherent problems in these optimizers arise when they deal with non-linear similarity metrics (derivative information must be estimated) and work on noisy input images, as we will handle later (Section 4.2). The application of several emerging evolutionary algorithms to the IR optimization process has caused an outstanding interest in order to solve the latter problems due to their global optimization techniques nature, as we will briefly depict in Section 3.

2.2. IR methods taxonomy

Our aim is not to present an extensive survey on IR methods. Nevertheless, we want to introduce the key concepts related to the IR methodology. During the last decades, many different taxonomies have been established to classify the huge amount of IR methods presented so far (Brown, 1992; Zitová and Flusser, 2003), considering different criteria: the image acquisition procedure, the search strategy guidelines, the search space definition, etc. One important criterion for our approach is based on the feature space characterization. IR methods can be classified as *voxel-based* and *feature-based*. While the formers directly operate with the whole input images, the latter approaches introduce a previous step: before the application of the registration process, a reduced subset of those more relevant features are extracted from the images. Since voxel-based methods can deal with a major amount of image information, they are considered as a *fine* registration, while feature-based methods achieve a *coarse* approximation due to the reduced data they take into account.

One important drawback in voxel-based approaches relies on the commonly used rectangular window for the correspondence estimation. If the images are deformed by complex transformations, this type of window will not be able to cover the same parts of the transformed scene and model images. Moreover, those cases where the window contains a smooth image region without any prominent details, will probably be incorrectly matched with other smooth image regions in the model image. To avoid such a scenario, Castellanos et al. (2004) introduce a successful technique that handles several levels of resolution, from coarse to fine, applying a GA to perform a global optimization by means of the normalized mutual information similarity metric. Nevertheless, the principal disadvantage of voxel-based methods come from those situations where there are changes on image illumination, bringing out the similarity metric offers unreliable measurements.

With the intention of avoiding many of the drawbacks related to voxel-based methods, the second approach is based on the extraction of prominent geometric primitives (*features*) in the images. A reliable feature detector must allow to properly compare feature sets by the invariance and accuracy of such a detector, that is, regardless changes in the geometry of the images, radiometric conditions, and appearance of noise. There are many different features that can be explored: (i) *region features* (Flusser and Suk, 1994), that, for example in satellite images, enclose water reservoirs, lakes or urban areas. The regions are often represented by their centers of gravity; (ii) *line features* representing general line segments (Ziou and Tabbone, 1998) or object contours (Maintz et al., 1996) (for example, anatomic structures in medical imaging applications). The correspondence between line segments is usually expressed by pairs of line ends or middle points; and (iii) *point features*, mainly consisting of methods working with line intersections, detection of local curvature discontinuities (Manjunath et al., 1996), and corners (Rohr, 2001). Corners are widely used as feature points due to their invariance to the image geometry and because they are well perceived by a human observer. Recently, Olague et al. have proposed a new parametric model (named *USEF*) able to provide the flexibility and generality for building any kind of complex corners (Olague and Hernández, 2005), and the authors have successfully improved its detection applying an hybrid evolutionary ridge regression approach (Olague et al., 2003).

The SS-based IR optimizer proposed in this contribution belongs to the latter feature-based approach and the features considered are prominent image points extracted from local curvature information (Monga et al., 1991) (see Section 5.1).

3. Evolutionary computation and image registration

An exhaustive review of the different EC approaches to the IR problem is out of the scope of our study. Nevertheless, we will mention some of their more important aspects in order to achieve a deep understanding of our work.

The first preliminary attempts to solve IR using EC can be found in the early eighties. Such an approach based on a GA was proposed in 1984 for the 2D case and applied to angiographic images (Fitzpatrick et al., 1984). Since this initial contribution, different authors solved the problem but we can still find important limitations in their approaches:

- The use of a binary coding to solve an inherent real coding optimization problem, with the precision depending on a given number of bits in the encoding (Garai and Chaudhuri, 2002; Yamany et al., 1999).
- The kind of GA considered, usually Holland's original proposal (Holland, 1975). This GA was proposed 30 years ago and it suffers from several drawbacks (namely, premature convergence to local optima), later solved by other genetic components and/or more advanced evolutionary algorithms establishing a proper search intensification–diversification tradeoff. The contributions in (Yamany et al., 1999; Garai and Chaudhuri, 2002)[1] are based on this classical GA.
- Many approaches only handle images suffering a translation and a rotation transformation (Garai and Chaudhuri, 2002; He and Narayana, 2002; Yamany et al., 1999), which is not the case in many real situations where at least the consideration of a uniform scaling is desirable. The resulting similarity transformation suits the registration of aerial and satellite images, bony structures in medical images, and brain multimodal images (Goshtasby, 2005).

In a recent work (Chow et al., 2004), the use of GAs with more suitable components to the current EC framework is considered such as a real coding scheme and a sophisticated restart mechanism (''dynamic boundary''). In spite of these improvements, there are some drawbacks in terms of accuracy, as the authors work with a smaller, randomly selected data set from scene images with a huge amount of data. Besides, although the algorithm aims at getting a quick registration estimation with the latter procedure, the efficiency could be reduced since it needs to perform a sort operation for each evaluation of the fitness function. As in many of the mentioned proposals, it also has the limitation of considering a transformation composed of a translation and a rotation.

Notice that we are tackling with the specific IR problem where the aim is to obtain the concrete f transformation function achieving the best overlapping between the scene and the model. A similar problem is the object shape alignment in pattern recognition where the goal is to decide whether two dissimilar images were originated from

[1] Nevertheless, this proposal is slightly improved respect to Holland's GA since it progressively adjusts the search space size and the mutation probability.

different items, or belonged to the same object but viewed from different camera positions; tackled with GAs in (Tsang, 1997). Likewise, in (Hill and Taylor, 1992) the application of GAs in model-based image interpretation is described. However, we will not consider these two latter approaches in the current contribution since they refer to a different problem than ours.

4. A fast and accurate scatter search algorithm for 3D IR

Our proposal is a feature-based approach to the IR problem. The aim is finding a near-optimal geometric transformation, competitive enough considering both time and accuracy criteria, when comparing to state-of-the-art methods. To do so, we will use an efficient stochastic optimization technique named SS (Laguna and Martí, 2003). Although feature-based methods achieve a coarse IR estimation, we have chosen such a feature-based approach since the smaller the amount of image data to be managed, the easier the application of different local and global search heuristics, in order to achieve fast and accurate results (the final goal of our ad-hoc SS-based IR optimizer design).

4.1. Basis of scatter search

SS fundamentals were originally proposed by Glover (1977) and have been later developed in some texts like Laguna and Martí (2003). The main idea of this technique is based on a *systematic* combination between solutions (instead of a randomized one like that usually done in GAs) taken from a considerably reduced evolved pool of solutions named *Reference set* (between five and 10 times lower than usual GA population sizes). This way, an efficient and accurate search process is encouraged thanks to the latter and to other innovative components we will describe later. The general SS approach is graphically shown in Fig. 2.

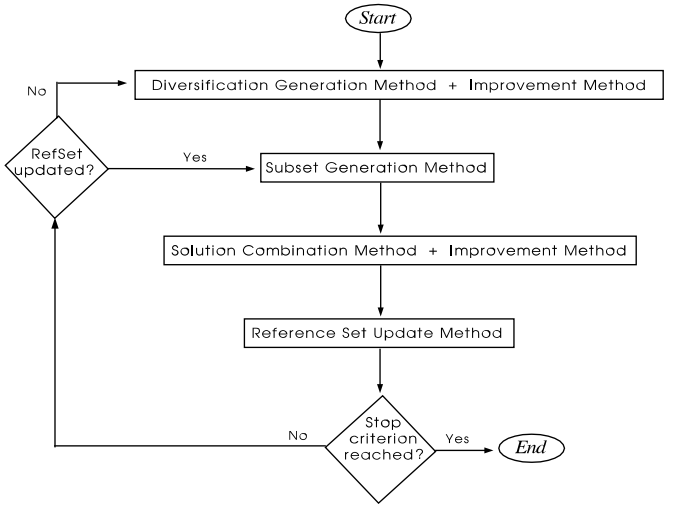

Fig. 2. The control diagram of SS.

4.2. Coding scheme and objective function

As coding scheme, the 3D similarity transformation f is determined fixing eight real-coded parameters which will be the ones we will look for. That is: a rotation $R = (\theta, Axis_x, Axis_y, Axis_z)$, a translation $\vec{t} = (t_x, t_y, t_z)$ and an uniform scaling s, where θ and $Axis$ define the 3D rotation given by an angle and an axis, respectively. Moreover, for a more suitable rotation representation, we consider quaternions instead of the three classical Euler matrices representation that suffers from the problem of *gimbal lock* (Shoemake, 1985).

In this contribution, we propose a new design for the IR Similarity metric, i.e., the objective function (noted as F). We will deal with a maximization problem similar to those used in the IR literature but adding a second term that helps to achieving the estimation of the uniform scaling transformation parameter, few times considered before by other authors, as shown follows:

$$F(f, I_s, I_m) = \omega_1 \cdot \left(\frac{1}{1 + \sum_{i=1}^{N} \|(sR\vec{p}_i + \vec{t}) - \vec{p}'_j\|^2} \right) + \omega_2 \cdot \left(\frac{1}{1 + |\rho_c^s - \rho^m|} \right) \quad (1)$$

where I_s and I_m are the scene and model images; f is the transformation encoded in the evaluated solution; $\vec{p}_i$ is the ith 3D point from the scene and $\vec{p}'_j$ is its corresponding nearest point in the model obtained with the GCP structure; ω_1 and ω_2 ($\omega_1 + \omega_2 = 1$) weight the importance of each function term; ρ_c^s is the radius of the sphere wrapping up the scene image transformed with the current f; and ρ^m is the radius of the sphere wrapping up the model image. Note that F maximizes to 1.0 for a rarely perfect fit.

In order to speed up the GCP structure computation (Yamany et al., 1999), we have performed an improvement using a Kd-tree structure (Zhang, 1994) for the GCP cell initialization, instead of using the brute force search. So, GCP achieves the closest point search in constant time, except for those transformed scene points that fall outside the grid. In those cases, a Kd-tree search is performed.

Likewise, the second term of F is needed in order to properly estimate scaling changes. Note that, since we are dealing with a maximization problem, if this term is not considered, the lower the s scaling factor obtained, the better the estimation. Hence, if $s \simeq 0$ then a "false" maximum of F is achieved. This leads us to enforce the s factor not to be null and to define a proper range of values for it (introducing the second term of F).

4.3. SS-based 3D IR implementation

The fact that the mechanisms within SS are not restricted to a single uniform design allows the exploration of strategic possibilities that may prove effective in a particular implementation. Of the five methods in the SS methodology, only four are strictly required. The improve-

```
P ← ∅
While (|P| < PSize) do
    Obtain a new solution x generated by the Diversification Generation Method
    Improve x with the Improvement Method generating the solution x'
    If x' ∉ P Then P ← P ∪ {x'}
Sort the solutions in P according to their objective function value (the best overall solution in P, that one with the
highest F value, is the first in such list). Add the first b solutions from P to RefSet

While (not reached the stop criterion) do
    NewElements ← True
    Pool ← ∅
    While (NewElements) and (not reached the stop condition) do
        Generate Subsets with the Subset Generation Method
        NewElements ← False
        While (Subsets ≠ ∅) do
            Select the next subset s from Subsets and delete it from Subsets
            Apply the Solution Combination Method on s to obtain a new solution x
                If (F(x) is higher than the F value of the median-solution ∈ RefSet) Then
                    Apply the Improvement Method to the solution x with a probability of
                    0.0625 [a] to obtain the solution x'
                Else x' ← x
                Add x' to Pool
        Apply the Reference Set Update Method selecting the best b solutions in RefSet ∪ Pool
        If (RefSet has at last one new solution) Then NewElements ← True
    If (not reached the stop criterion) Then
        Build a new set P using the Diversification Generation Method
        Replace the worst b − 1 solutions from RefSet with the best b − 1 solutions from P
```

[a] The use of such a probability value was justified in (Hart, 1994) and successfully applied in (Lozano et al., 2004) in order to achieve a quick convergence to good solutions of the global SS procedure.

Fig. 3. Pseudocode of the SS-based 3D IR optimizer (see also Hart (1994) and Lozano et al. (2004)).

ment method is usually needed if high quality outcomes are desired, but a SS procedure can be implemented without it. Next, we will briefly describe the specific design of each component of our SS-based 3D IR method outlined in Fig. 3, where P denotes the initial set of solutions generated with the *diversification generation method* (with *Psize* being the size of P), the reference set is noted as *RefSet* (with b being its size, usually significantly lower than *Psize*), and *Pool* is the set of trial solutions constructed with the *combination* and *improvement methods* each iteration.

4.3.1. Diversification generation method

This method makes use of a controlled randomization based on frequency memory to generate an initial set P of *Psize* diverse solutions (Glover et al., 2003). We carry out this by dividing the range of each variable (in our case, each one of the eight similarity transformation parameters) into four sub-ranges of equal size. A solution will be constructed in two steps. First, a sub-range is randomly selected for each variable, where the probability of choosing a sub-range is inversely proportional to its frequency count. Initially, the frequency count for each variable sub-range is set to one and the number of times a sub-range j has been chosen to generate a value for variable i in a solution is accumulated in *frequency_count*(i,j). Then, as second step, a value is randomly generated within the selected sub-range. Finally, the *improvement method* is applied on the *Psize* solutions generated and the best b of them compose the initial *RefSet*.

4.3.2. Improvement method

The improvement method is based on Solis and Wets' optimization algorithm (Solis and Wets, 1981), which has the advantage of not requiring to compute the gradient direction in order to operate. This classical local search algorithm uses fixed variances which are initially and uniformly one. These variances are used for probabilistically determining the change to be applied on a particular state variable. They are either doubled or halved during the run, depending on the number of consecutive failed or successful moves. On the other hand, we also considered the use of the Nelder and Mead's Simplex Method (Nelder and Mead, 1965) but later discarded it because it required a larger number of objective function evaluations, to achieve good results.

4.3.3. Subset generation method

This method generates a collection of solution subsets (noted as *Subsets* in Fig. 3) of the reference set as a basis for creating new combined solutions. In our implementation, the subsets are composed of all the possible pairs of solutions in *RefSet*, so $\frac{b\cdot(b-1)}{2}$ different subsets are generated.

4.3.4. Solution combination method

It is based on the use of the BLX-α crossover operator (Eshelman, 1993), commonly used in real-coded GAs. This mechanism for combination obtains a trial solution, $x = (h_1, \ldots, h_k, \ldots, h_l)$ (with $l = 8$ being the number of parameters of the similarity transformation and h_k a given value for such kth variable) from the two parent solutions $x^1 = (c_1^1, \ldots, c_l^1)$ and $x^2 = (c_1^2, \ldots, c_l^2)$, composing a given subset s (see Fig. 3), by uniformly generating a random value for each variable h_k in the interval $[c_{\min} - I \cdot \alpha, c_{\max} + I \cdot \alpha]$, with $c_{\max} = \max(c_k^1, c_k^2)$, $c_{\min} = \min(c_k^1, c_k^2)$, and $I = c_{\max} - c_{\min}$. Hence, the parameter α allows us to make this crossover as disruptive as desired. Such combination method was successfully incorporated to SS in (Herrera et al., 2006).

The solution obtained by the BLX-α is then selectively optimized by the *improvement method* and included in the *Pool*, as shown in Fig. 3.

4.3.5. Reference set update method

RefSet is updated to be composed of the b best solutions in $RefSet \cup Pool$ following a static strategy (first, the *Pool* set is built and then the updating is made) (Laguna and Martí, 2003).

5. Experiments

We present a number of experiments to study the performance of our proposal. As a benchmark, the results obtained by our SS algorithm for the 3D IR problem will be compared against those obtained by the improved iterative closest point matching (*I-ICP*) algorithm proposed in (Liu, 2004), and by two other evolutionary approaches: the binary-coded GA (*BGA*) proposed by Yamany et al. (1999), and the fast real-coded dynamic GA (*DGA*) introduced by Chow et al. (2004). The three algorithms maintain their original form and just the second term of our objective function (see Eq. (1)) has been added to the original fitness functions of the two GAs in order to allow them to deal with the uniform scaling factor, not considered in their original proposals (thus making possible our experimental comparison).

5.1. Image registration problems considered

We work on a number of registration problems for six different 3D images which have suffered the same three similarity transformations (noted as T_1, T_2 and T_3 in Table 1), to be estimated by the different 3D IR algorithms applied.

The first is a synthetic image named as I_{Skull} and composed of 1306 control points, originally considered in (Chow et al., 2004). On the other hand, we have also used a real magnetic resonance image (MRI) [presented in (Thirion and Gourdon, 1995), and considered in our previous works (Cordón and Damas, in press; Cordón et al., 2003)] named as I_{Brain^1}, and other three realistic T1 MRIs of a normal brain from the *BrainWeb* database at McGill University (Kwan et al., 1999), named as I_{Brain^2}, I_{Brain^3} and I_{Brain^4}, respectively. Each one of the four MRIs were originally composed of more than thirty thousands data points but subsequently reduced applying a preprocessing to extract their representative points by using a 3D crest lines edge detector (Monga et al., 1991), in order to accelerate the algorithmic convergence of each IR method. The resulting MRIs are comprised by 9108, 583, 348 and 284 points, respectively. These five images are shown in Fig. 4.

In order to test the performance of our proposal when facing noisy and occluded situations, the I_{Brain^3} and I_{Brain^4} images inherently present a multiple sclerosis lesion with 1% and 5% of Gaussian noise, respectively. Moreover, the 30% of the I_{Brain^1} image points have been disturbed by a normal distribution with a standard deviation $\sigma = 0.05$, thus generating the last image, $I_{\text{Brain}^{1'}}$.

Table 1
Applied transformations to every 3D test image

	θ	$Axis_x$	$Axis_y$	$Axis_z$	t_x	t_y	t_z	s
T_1	125.7	0.742	0.636	−0.212	17.5	−25.8	−43	0.7
T_2	215.4	−0.505	0.303	−0.808	−48.7	20	52.5	1
T_3	95	−0.768	−0.383	0.512	−8	65.2	37.7	1.5

5.2. Parameter settings

The evolutionary methods are run for the same fixed time of 40 s on a 900 MHz. AMD processor. However, the I-ICP algorithm is run until it achieves its convergence threshold (what makes it last up to 3 min in every instance considering I_{Brain^1} and $I_{\text{Brain}^{1'}}$), due to the fact that it is considered as a baseline for the performance of the evolutionary approaches.

In order to avoid execution dependence, 30 different runs of each IR algorithm have been performed, except for the deterministic I-ICP that only requires one run. The BGA encodes each parameter with 15 bits. Crossover probability is $P_c = 0.6$ and three different values are tested for the mutation probability ($P_m = \{0.01, 0.05, 0.1\}$). The population size is 100. The best results obtained for BGA regardless the parameter values are reported. On the other hand, the DGA works with 500 individuals and with 300 scene image points, as indicated in (Chow et al., 2004). Finally, for the SS, the initial diverse set P comprises $Psize = 30$ solutions and the *RefSet* is composed of the $b = 12$ best ones of them. BLX-α is applied with $\alpha = 1$ (Lozano et al., 2004), while the *improvement method* is selectively applied during 40 evaluations each time. The values chosen for the objective function weights ω_1 and ω_2 were 0.75 and 0.25, respectively.[2]

5.3. Analysis of results

Notice that all statistics in this section are based on a typical error measure in the IR field, the *mean square error* (MSE), given by

$$\text{MSE} = \frac{\sum_{i=1}^{N} \|f(\vec{p}_i) - \vec{p}'_j\|^2}{N}$$

where f is the estimated registration function, $\vec{p}_i$ are the scene points, and $\vec{p}'_j$ are the model points matching the scene ones (the closest to the formers).

Table 2 and Fig. 5 show the performance of the different IR algorithms applied, respect to the five IR instances for the six test images and the three transformations considered. The second group of rows are referred to the noisy/occluding scenarios.

[2] Different weight combinations were tested in a preliminary experimentation, achieving similar results, thus showing the SS robustness.

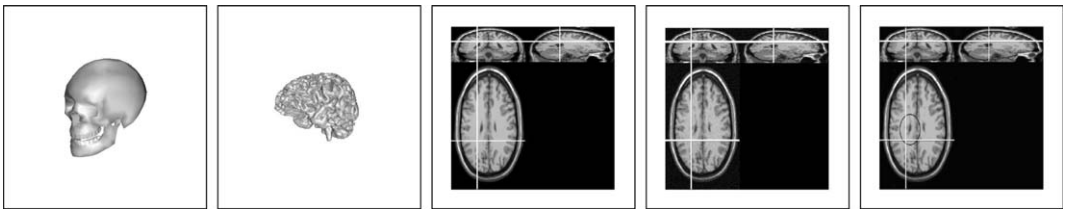

Fig. 4. Five of the six original images: I_{Skull}, I_{Brain^1}, I_{Brain^2}, I_{Brain^3} and I_{Brain^4}.

Table 2
MSE of the f estimations found by each of the IR methods (*statistics of thirty different runs for each evolutionary IR method*), considering the six test images and the three known transformations (Table 1)

		Best			Median			Mean			Standard deviation		
		T_1	T_2	T_3	T_1	T_2	T_3	T_1	T_2	T_3	T_1	T_2	T_3
I_{Skull} vs. $f_{T_i}(I_{\text{Skull}})$	SS	**0**	**0**	**0**	0	3e−5	0	2e−3	**3e−3**	**5e−3**	3e−3	4e−3	8e−3
	BGA	6e−7	6e−5	3e−6	1e−3	0.01	0.01	**1.2e−3**	0.06	0.01	1.3e−3	0.2	0.01
	DGA	0.03	0.02	0.03	0.09	0.2	0.2	0.21	0.43	0.2	0.44	0.57	0.11
	I-ICP	0.45	0.04	0.22	–	–	–	–	–	–	–	–	–
I_{Brain^1} vs. $f_{T_i}(I_{\text{Brain}^1})$	SS	**2e−4**	**2e−4**	**1e−4**	9e−4	0.02	1e−3	**0.35**	**24.4**	**6e−3**	1.6	32	0.01
	BGA	0.6	0.8	0.01	5.89	23.7	17.38	11.3	32.1	37.8	11.1	27.4	46.9
	DGA	22.4	59.8	101.6	46.1	126.6	238.7	54.2	145.9	245.6	29.4	60.0	86.6
	DGA*	44.2	33.2	137.7	66	133.1	299.2	69.3	129.1	300.7	18.2	40.9	97
	I-ICP	3572	2496	16239	–	–	–	–	–	–	–	–	–
Noisy/occluding experimentation													
I_{Brain^2} vs. $f_{T_i}(I_{\text{Brain}^3})$	SS	**32.1**	**64.7**	**146.2**	32.2	65.1	146.9	**32.3**	**87.3**	**152.3**	0.3	31.5	27.1
	BGA	32.3	65.2	147.09	34.9	133.7	163.8	52.1	129.2	196.4	27.4	34.5	73.8
	DGA	128.4	265.7	477.7	309.2	441.6	892.1	322.7	593.7	1171	157.1	305.8	679.4
	I-ICP	755.4	534.1	485.3	–	–	–	–	–	–	–	–	
I_{Brain^2} vs. $f_{T_i}(I_{\text{Brain}^4})$	SS	**23.6**	**48.1**	**108.1**	23.8	48.3	108.2	**24.6**	**65.4**	**115.8**	4.4	24.2	28.9
	BGA	23.9	48.3	108.7	26.1	99.6	122.2	35.3	89.2	177.3	15.3	30.1	87.6
	DGA	63.2	177.3	501.1	254.7	413.4	962.7	245.4	481.2	1058	103.8	281.4	505.7
	I-ICP	1779	1706	610.2	–	–	–	–	–	–	–	–	
I_{Brain^1} vs. $f_{T_i}(I_{\text{Brain}^{1'}})$	SS	**17.5**	**32.2**	**78.9**	17.6	32.6	79.7	**20**	**42.2**	**83**	6.2	12	15.6
	BGA	17.6	32.3	79.4	21.4	56.7	87.3	24.1	50.1	98.7	6.6	13.1	22.7
	DGA	36	77.7	124.6	74.1	187	267.3	90.6	210.4	290.4	43.9	97	123.8
	I-ICP	2599	294.7	10698	–	–	–	–	–	–	–	–	

Note that the image model is noted by $f_{T_i}(image)$ and the best estimations are highlighted using bold font.

Analyzing the results obtained, we can see how our SS-based proposal achieves the most accurate results in the best, median and mean values. Although the BGA obtains similar results as regards the best values, our approach is significantly better in view of the really smaller median and mean values. The differences are even more outstanding when dealing with the real noise-free MRI (I_{Brain^1}). The robustness of the SS algorithm is shown by the lowest standard deviation, mean and median values obtained, which allows us to highlight its quick convergence to high quality solutions in all the 30 runs performed considering a fixed run time of 40 s (thus achieving our goal of designing a fast IR algorithm). The quickness of our proposal is also emphasized by the convergence graphs shown in Fig. 6, which represent the average of the 30 runs performed by each of the three evolutionary-based techniques (SS, BGA and DGA) in the I_{Brain^1} vs. $f_{T_i}(I_{\text{Brain}^1})$ scenario.

The behavior presented by each IR algorithm considered under noisy/occlusion conditions (shown in the last three rows of Table 2) is similar to that from noise/occlusion-free instances. Our proposal outperforms the remaining methods, demonstrating its robustness under noisy/occluding scenarios.

We can see that both the SS and BGA approaches outperform I-ICP in the five IR instances, and could be noticed how such a deterministic approach obtains a very high MSE value for most of the instances. The poor estimation obtained by I-ICP is due to the fact that the uniform scaling parameter it obtains is badly estimated. It could be seen how, for the three transformations, the MSE value proportionally increases with the scaling factor (see Table 1).

Notice that, the BGA performs better than the DGA in spite the latter deals with only 300 data points, randomly

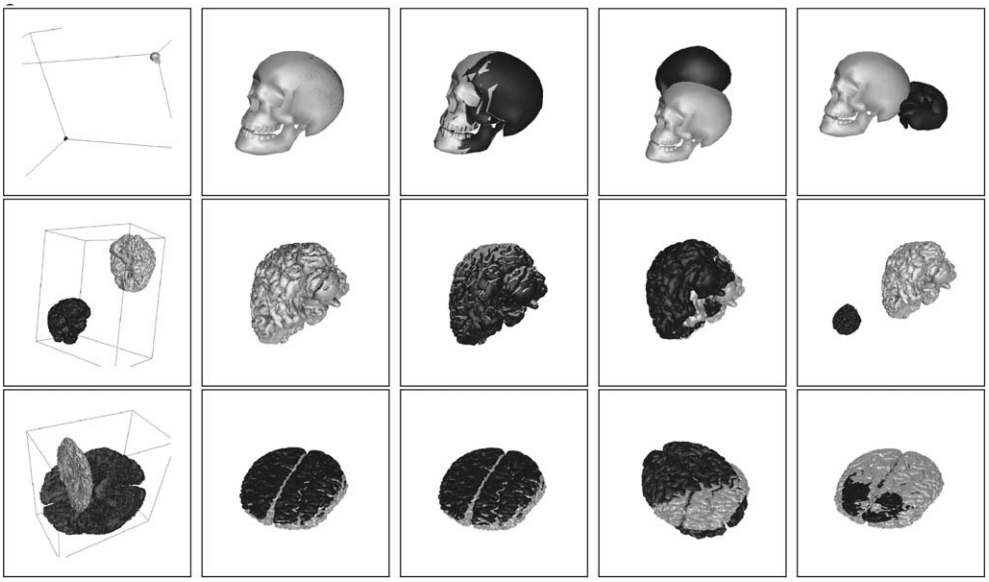

Fig. 5. From top to bottom, the first cell at the first, second and third row show the I_{Skull} vs. $f_{T_1}(I_{\text{Skull}})$, I_{Brain^1} vs. $f_{T_2}(I_{\text{Brain}^1})$ and I_{Brain^2} vs. $f_{T_3}(I_{\text{Brain}^4})$ scenarios, and from left to right starting in the second cell in each row, the 3D-rendering of the best SS, BGA, DGA and I-ICP IR estimations for the previous scenarios is depicted.

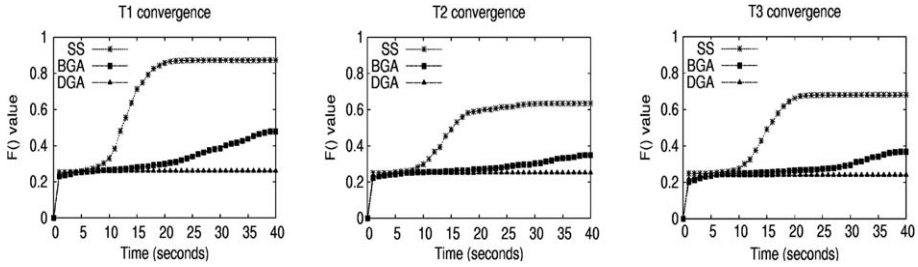

Fig. 6. Convergence graphs of the three evolutionary algorithms when estimating the three registration transformations for instance I_{Brain^1} vs. $f_{T_i}(I_{\text{Brain}^1})$ (the curves shown are averaged between the 30 runs performed).

selected in the scene image before the run to achieve a faster process, and with a real coding. It could be due to the fact that the BGA has crossover and mutation operators more appropriate for the handled representation, furthermore including the GCP structure that speeds up the overall process, instead of using a less efficient Kd-tree structure as done by the DGA. Besides, the results in the second row of Table 2 labelled as DGA* show the outcomes carried out by the DGA in the same CPU time when dealing with the 10% of the scene data points (910 points) for the I_{Brain^1} vs. $f_{T_i}(I_{\text{Brain}^1})$ instance. It can be viewed how such data point increase does not improve the performance obtained dealing with a lower number of data points since the algorithm would need more CPU time to compute the double of Kd-tree searches to obtain more accurate results.

Finally, Table 3 includes the transformation parameters estimated by the two most accurate algorithms, SS and BGA, for the most complex IR instance, to remark their similarity with the ground truth transformations in Table 1.

Table 3
The best parameter estimations for the I_{Brain^1} vs. $f_{T_i}(I_{\text{Brain}^{1'}})$ instance

		α	$Axis_x$	$Axis_y$	$Axis_z$	t_x	t_y	t_z	s
T_1	SS	126.3	0.733	0.64	−0.229	16.8	−25.6	−42.8	0.83
	BGA	124.4	0.73	0.639	−0.241	17.9	−25.9	−43.4	0.83
T_2	SS	216.6	−0.512	0.293	−0.808	−46.2	20.5	51.8	1.16
	BGA	213.8	−0.524	0.285	−0.803	−44.6	18.9	52	1.16
T_3	SS	96.1	−0.765	−0.38	0.52	−8.7	64.9	40.1	1.7
	BGA	97.9	−0.777	−0.378	0.504	−9.3	66.3	40.5	1.8

6. Concluding remarks and future works

In this paper, we have introduced the use of a novel evolutionary framework, SS, as a new IR optimizer for the 3D IR problem handling with similarity transformations. Having in mind the interesting properties and the recent successful outcomes achieved by the former strategy in other global optimization problems (Laguna and Martí, 2003), our starting point was that the combined use of the SS components and the way they are assembled, on the one hand, and the improvement of both data structures and crucial process for the IR problem, on the other hand, could solve the lacks presented by previous GA-based IR approaches and classical ones as ICP, thus obtaining a faster, more suitable and more accurate automatic tool for this task.

In view of the experimental results obtained in five 3D IR instances—using one synthetic and five MRIs, our proposal performs a better global search than the most representative existing GA-based techniques, as well as than the recently improved ICP algorithm. The performance of the SS-based approach is especially remarkable in the real-world MRI instance, composed of more than 9000 points, as regards the reduced run time considered (40 s).

As future works, we think on incorporating more advanced variants to the SS algorithm to reduce even more its run time and achieve more accurate results. It will also be interesting to extend our proposal to other scenarios such as voxel-based multimodality IR problems (see Section 2.2), which would only require minor changes over the proposed design, such as modifying the objective function or the registration transformation f (affine, elastic, etc.).

Acknowledgement

The authors would like to thank the anonymous referees for their valuable comments that allowed them to highly improve the paper quality.

References

Bäck, T., Fogel, D.B., Michalewicz, Z. (Eds.), 1997. Handbook of Evolutionary Computation. IOP Publishing Ltd. and Oxford University Press.

Besl, P.J., McKay, N.D., 1992. A method for registration of 3-D shapes. IEEE Trans. Pattern Anal. Machine Intell. 14, 239–256.

Brown, L.G., 1992. A survey of image registration techniques. ACM Comput. Surveys 24 (4), 325–376.

Castellanos, N.P., Angel, P.L.D., Medina, V., 2004. Nonrigid medical image registration technique as a composition of local warpings. Pattern Recognition 37, 2141–2154.

Chow, C.K., Tsui, H.T., Lee, T., 2004. Surface registration using a dynamic genetic algorithm. Pattern Recognition 37, 105–117.

Cordón, O., Damas, S. 2005. Image registration with iterated local search. Journal of Heuristics, in press.

Cordón, O., Damas, S., Santamaría, J., 2003. A CHC evolutionary algorithm for 3D image registration. In: Bilgic, T., Baets, B.D., Bogazici, O. (Eds.), Lecture Notes in Artificial Intelligence, 2715. Springer, Heidelberg, pp. 404–411.

Eshelman, L.J., 1993. Real-coded genetic algorithms and interval schemata. In: Whitley, L.D. (Ed.), Foundations of Genetic Algorithms, 2. Morgan Kaufmann, San Mateo, pp. 187–202.

Fitzpatrick, J.M., Grefenstette, J.J., Van Gucht, D. 1984. Image registration by genetic search, In: IEEE Southeast Conference, Louisville, USA, pp. 460–464.

Flusser, J., Suk, T., 1994. A moment-based approach to registration of images with affine geometric distortion. IEEE Trans. Geosci. Remote Sensing 32, 382–387.

Garai, G., Chaudhuri, B.B., 2002. A cascaded genetic algorithm for efficient optimization and pattern matching. Image Vision Comput. 20, 265–277.

Glover, F., 1977. Heuristic for integer programming using surrogate constraints. Decision Sciences 8, 156–166.

Glover, F., Laguna, M., Martí, R., 2003. Scatter search. In: Ghosh, A., Tsutsui, S. (Eds.), Advances in Evolutionary Computation: Theory and Applications. Springer-Verlag, New York, pp. 519–537.

Goshtasby, A.A., 2005. 2-D and 3-D Image Registration for Medical, Remote Sensing, and Industrial Applications. Wiley Interscience.

Han, K.P., Song, K.W., Chung, E.Y., Cho, S.J., Ha, Y.H., 2001. Stereo matching using genetic algorithm with adaptive chromosomes. Pattern Recognition 34 (9), 1729–1740.

Hart, W.E., 1994. Adaptive Global Optimization with Local Search. Ph.D. Thesis, University of California, San Diego, California.

He, R., Narayana, P.A., 2002. Global optimization of mutual information: application to three-dimensional retrospective registration of magnetic resonance images. Comput. Med. Imaging Graph. 26, 277–292.

Herrera, F., Lozano, M., Molina, D., 2006. Continuous scatter search: an analysis of the integration of some combination methods and improvement strategies. Eur. J. Operat. Res. 169 (2), 450–476.

Hill, A., Taylor, C.J., 1992. Model-based image interpretation using genetic algorithms. Image Vision Comput. 10 (5), 295–300.

Holland, J.H., 1975. Adaptation in Natural and Artificial Systems. The University of Michigan Press, Ann Arbor.

Kwan, R.K.S., Evans, A.C., Pike, G.B., 1999. MRI simulation-based evaluation of image-processing and classification methods. IEEE Trans. Med. Imaging 18 (11), 1085–1097.

Laguna, M., Martí, R., 2003. Scatter Search: Methodology and Implementations in C. Kluwer Academic Publishers, Boston.

Liu, Y., 2004. Improving ICP with easy implementation for free form surface matching. Pattern Recognition 37 (2), 211–226.

Lozano, M., Herrera, F., Krasnogor, N., Molina, D., 2004. Real-coded memetic algorithms with crossover hill-climbing. Evolution. Comput. 12 (3), 273–302.

Maintz, J.B.A., van den Elsen, P.A., Viergever, M.A., 1996. Evaluation on ridge seeking operators for multimodality medical image matching. IEEE Trans. Pattern Anal. Machine Intell. 18, 353–365.

Manjunath, B.S., Shekhar, C., Chellapa, R., 1996. A new approach to image feature detection with applications. Pattern Recognition 29, 627–640.

Monga, O., Deriche, R., Malandain, G., Cocquerez, J.P., 1991. Recursive filtering and edge tracking: two primary tools for 3D edge detection. Image Vision Comput. 9 (4), 203–214.

Nelder, J.A., Mead, R., 1965. A simplex method for function minimization. Comput. J. 7 (4), 308–313.

Olague, G., Hernández, B., 2005. A new accurate and flexible model based multi-corner detector for measurement and recognition. Pattern Recognition Lett. 26, 27–41.

Olague, G., Hernández, B., Dunn, E. 2003. Hybrid evolutionary ridge regression approach for high-accurate corner extraction. In: IEEE Conference on Computer Vision and Pattern Recognition, Madison, USA, June 16–23, pp. 744–749.

Rohr, K., 2001. Landmark-based image analysis: using geometric and intensity modelsComputational Imaging and Vision Series, vol. 21. Kluwer Academic Publishers, Dordrecht.

Shoemake, K., 1985. Animating rotation with quaternion curves. ACM SIGGRAPH'85 19 (3), 245–254, San Francisco, July 22–26.

Solis, F.J., Wets, R.J.B., 1981. Minimization by random search techniques. Math. Operat. Res. 6, 19–30.

Thirion, J.P., Gourdon, A., 1995. Computing the differential characteristics of iso-intensity surfaces. Comput. Vision Image Understand. 61 (2), 190–202.

Tsang, P.W.M., 1997. A genetic algorithm for aligning object shapes. Image Vision Comput. 15 (11), 819–831.

Yamany, S.M., Ahmed, M.N., Farag, A.A., 1999. A new genetic-based technique for matching 3D curves and surfaces. Pattern Recognition 32, 1817–1820.

Zhang, Z., 1994. Iterative point matching for registration of free-form curves and surfaces. Internat. J. Comput. Vision 13 (2), 119–152.

Ziou, D., Tabbone, S., 1998. Edge detection techniques—an overview. Internat. J. Pattern Recognition Image Anal. 8, 537–559.

Zitová, B., Flusser, J., 2003. Image registration methods: a survey. Image Vision Comput. 21, 977–1000.